

Supplementary material:

The EMEP MSC-W chemical transport model - Part I: Model description

D. Simpson^{1,2}, A. Benedictow¹, H. Berge¹, R. Bergström^{3,4},
L.D. Emberson⁵, H. Fagerli¹, G.D. Hayman⁶, M. Gauss¹,
J.E. Jonson¹, M.E. Jenkin⁷, A. Nyíri¹, C. Richter⁸, V.S.
Semeena¹, S. Tsyro¹, J.-P. Tuovinen⁹, Á. Valdebenito¹, &
P. Wind¹

A1 EMEP model revision history

Table A1. Summary of major EMEP model versions

Revision	Label	Date	Main changes
rv2.5		Jul 2006	Used for IIASA (GAINS) source-receptor matrices.
rv3.0		Feb. 2008	First public-domain release.
rv3.2			Included various small changes, e.g. to vegetation parameters, and numerous technical changes. Improved deposition scheme, including co-deposition for SO ₂ , revised particle deposition scheme, daily snow instead of climatological. Code revisions for more flexible grids and global scale.
rv3.4		2009	Additional chemical schemes implemented, EmChem09 scheme developed, Forecast model versions implemented.
rv3.6		2010	Boundary layer physics updates, convection routine added.
rv3.8	2011-05	May 2011	Second public-domain. Major revisions in: Aerosol dry deposition methodology, also revised sub-cloud scavenging; Biogenic VOC emission methods, rates; added cumulus scheme; ECMWF IFS model replaces PARLAM/HIRLAM NWPs as default meteorological driver;
rv3.9		Nov 2011	Major revisions: pH dependence of sulphate formation; added organic aerosol and SOA formation; use of daily FINNv1 forest fire module; changed temporal variations for sectors SNAP-1 (changing winter/summer ratios) and SNAP-2 (degree-days);
rv4.0	2012-YY	Early 2012	Third public-domain.

Many changes are continuous, for example there is an ongoing process to make the model more flexible with respect to meteorological drivers, chemical schemes, grid-projection, nesting and boundary conditions. The vertical coordinate scheme has been revised, and where possible global databases are being implemented (for example forest fires) for use by all model domains.

A2 Physical formulation and Numerics, additional information

The main paper has dealt with the physical and chemical formulation of the model. Here we address some of the numerical and computational details associated with the model structure.

A2.1 Convection

Numerical implementation of the convection scheme is described in Jonson et al. (2010b). We define the mass (per square meter) of a pollutant in the layer k as $\frac{\chi \Delta_k P}{g}$ where χ is the mass mixing ratio of a pollutant, $\Delta_k P$ is the pressure difference between the bottom and the top of the layer and g is the gravitational constant. The advantage of this formulation compared to using density times Δz , is that it is not dependent on a particular definition of the vertical coordinates.

We assume that the convective fluxes leaving the layer k through the top (cf. Fig. 3), F_k , are given by the meteorological driver. For **updrafts**, the process starts at surface (largest k). If $\Delta_k F = F_k - F_{k+1} > 0$, the pollutants are transported from the environment towards the cloud core (elevator). The mass of the pollutant removed from a grid cell and put into the core in layer k during time Δt , is given by $\chi_{grid} \Delta_k F \Delta t$, and the new mixing ratio becomes:

$$\chi_{grid}^{t+\Delta t} = \chi_{grid}^t - \chi_{grid}^t \frac{g \Delta_k F \Delta t}{\Delta_k P} \quad (\text{A1})$$

In this formulation $\Delta_k P$ is kept constant during the convection process. The mixing ratio of the pollutant in the cloud core becomes:

$$\chi_{core}^{t+\Delta t} = \chi_{core}^t + \chi_{grid}^t \frac{g \Delta_k F \Delta t}{\Delta_k P} \quad (\text{A2})$$

If mass is transported from the cloud core towards the grid cell, the proportion of pollutants removed from the core is given by $\frac{F_{k+1} - F_k}{F_{k+1}}$ and the new mixing ratios become

$$\chi_{grid}^{t+\Delta t} = \chi_{grid}^t + \chi_{core}^t \frac{F_{k+1} - F_k}{F_{k+1}} \quad (\text{A3})$$

$$\chi_{core}^{t+\Delta t} = \chi_{core}^t - \chi_{core}^t \frac{F_{k+1} - F_k}{F_{k+1}} \quad (\text{A4})$$

The pollutant in the core is then lifted to the next level:

$$\chi_{core(k-1)}^t = \chi_{core(k)}^{t+\Delta t} \frac{\Delta_{k+1} P}{\Delta_k P} \quad (\text{A5})$$

and the process is iterated until the top is reached.

A corresponding calculation for the downward fluxes is performed, starting from top and continuing down to the surface. After these detrainment and entrainment processes, the total mass of pollutants will be conserved, however there will be an imbalance between the quantity of air having entered and left the individual grid cells, because the large scale subsidence has not yet been accounted for. In order to mimic the subsidence process, we perform the same procedure starting with $\chi = 1$ at all levels, which will account for the modelled transport of ‘‘pure air’’.

The mass in a specific level obtained, $\frac{\chi \Delta_k P}{g}$ will then give a measure of the excess or deficiency of air. The air masses are then redistributed along the vertical column. The levels are filled successively starting from above until the original masses are recovered. The pollutants follow the same pattern.

A2.2 Time-step control

The numerical solution of the advection requires that the so-called Courant number does not exceed 1. The Courant (or CFL) number CU_0 is defined as $\frac{\Delta t}{\Delta x} |u|$ where u is wind-speed. This ensures that material from one grid cell can not be advected beyond the borders of its downwind neighbour. To take into account for a variable horizontal grid size, this expression must be scaled by the map factor. If the Courant number is exceeded the advection timestep is adjusted for different rows or columns where needed. The time step for the vertical advection can also be different from the time step in the horizontal directions, but all elementary time steps for the one dimensional advection have to be an integer fraction of Δt_{advect} . A too low Courant number will lead to an undesired increase in numerical diffusion and also an increase in CPU requirements.

For each row j and vertical level k , a maximum value for the time-step Δt in direction x is derived; the following expression is evaluated over all grid cells in the row:

$$\Delta t_{max}(j,k) \leq \frac{\Delta x}{\max(m^2 \frac{u(i,j,k)}{m_y(i,j)}, 0) - \min(m^2 \frac{u(i-1,j,k)}{m_y(i-1,j)}, 0)}$$

Where $m^2 = m_x(i,j) m_y(i,j)$, and m_x, m_y are map-factors (see also Sect. 2.2). Corresponding expressions for the y and vertical directions are used.

The time step is set to the same value for all cells in one single row in each horizontal direction, although they can be different for different rows and at different heights. See Wind et al. (2002) for further details of the time-step control system.

A2.3 Chemistry - numerical solution

As noted in section 7.10, the chemical equations are solved using the TWOSTEP algorithm tested by Verwer et al. (1996); Verwer and Simpson (1995). The formulae have however been re-arranged for greater computational efficiency (S. Unger. Pers. comm.), and so here we outline the algorithm as used in the model. Note that the notation here is different to that used by Verwer and Simpson (1995).

The algorithm used for the chemistry solutions are summarised below. From the main model, at the start (time t) of each advection time-step of length Δt_{advect} (typically 20 mins), we have 3-d arrays ($C_m^{3D}(i,j,k)$) of the chemical concentrations (in molecules cm^{-3}) of each species m , and of the chemical tendency, D_m (see below). Within one Δt_{advect} we use a number N_{chem} of chemical time-steps, of (uneven) width $\Delta t(n)$, where $n = 1 \dots N_{\text{chem}}$ (see below). We will use the notation $t(n) = t + \Delta t(1) + \dots + \Delta t(n)$. The scheme uses two values of concentrations, $C_m^{t(n-2)}$ and $C_m^{t(n-1)}$, to derive the next value $C_m^{t(n)}$.

1. Initialise time-step

$$\begin{aligned} C_m^{t(0)} &= C_m^{3D}(i,j,k) && \text{start with concentrations from 3-D fields at time } t \\ C_m^{t(-1)} &= C_m^{t(0)} - 1.5 D_m(i,j,k)\tau(1) && \text{Estimate based upon chemical tendency only. } (D_m \text{ and } \tau \text{ defined below, } D_m=0 \text{ when} \\ &&& \text{program starts).} \end{aligned}$$

2. Integration loop

For each chemical time-step (for $n = 1 \dots N_{\text{chem}}$) we then do:

$$\begin{aligned} C_m^* &= \alpha(n)C_m^{t(n-1)} - \beta(n)C_m^{t(n-2)} && \text{help variable} \\ C_m^{t(n)} &= C_m^{t(n-1)} + (C_m^{t(n-1)} - C_m^{t(n-2)})\gamma(n) && \text{First guess of new concs} \end{aligned}$$

For the general time-step n , coefficients α , β , γ , τ are calculated with:

$$\begin{aligned} \theta(n) &= \Delta t(n-1)/\Delta t(n) && (\text{for } n=1, \text{ we use } \theta(1)=1) \\ \beta(n) &= 1/(\theta(n)^2 + 2\theta(n)) \\ \alpha(n) &= (\theta(n) + 1)^2 \beta(n) \\ \tau(n) &= (\theta(n) + 1)/(\theta(n) + 2)) \Delta t(n) \\ \gamma(n) &= 1/\theta(n) \end{aligned}$$

2a. Calculation of $C_m^{t(n)}$

Following Verwer and Simpson (1995), a Gauss-Seidel integration procedure is then used, where for each species m , the production rate P_m , loss-rate L_m , and then the updated concentrations $C_m^{t(n)}$ are calculated in turn. The updated concentration for the iteration is then obtained using a Padé

approximation of the second order backward difference formula:

$$C_m^{t(n)} = \frac{C_m^* + \tau(n)P_m}{1 + \tau(n)L_m} \quad (\text{A6})$$

At each stage the the latest values of concentrations are used for all reactants. Step 2a, running through all species and using Eqn. A6 is iterated a number of times (from 1 to 3, see below). We then save the chemical tendencies and return the new concentrations of advected species to the 3-D fields:

$$D_m = (C_m^{t(n)} - C_m^{3D}(i,j,k)) / \Delta t_{\text{advec}}$$

$$C_m^{3D}(i,j,k) = C_m^{t(n)}$$

At present, with an advection time-step Δt_{advec} of 20 minutes (1200 s) the algorithm starts with five successive timesteps of $\Delta t_{\text{chem}}=20$ s followed by seven larger timesteps of just under 160 s. Compared with a fixed timestep, increasing timesteps has been found more efficient, since at the start of the process the system is further away from a steady-state situation. This scheme improves with iteration. In the 4 layers near the ground, where emission and usually reaction tendencies are highest, we perform 3 iterations each timestep. Above this, 2 iterations are performed, except for the uppermost 6 layers where 1 iteration is used.

A2.4 Parallel structure and CPU requirements

In order to produce results covering several years and several different situations, the model requires large computer resources. The program code is written in Fortran 90/95. The structure of the program is designed to allow for efficient parallelization on a system with distributed memory.

The horizontal grid is divided into a number of subdomains and each subdomain is assigned to a processor. Each processor holds only the data for its own subdomain. Because of this structure, the communication between the processors is kept to a minimum.

Still the advection routines fundamentally require information to be passed between processors. An additional limitation of the level of parallelity which can be achieved is that all input/output is currently done on one processor, and thus requires information to be passed between the processors. The input/output of data is also a limitation of the level of parallelity which can be achieved. The meteorological data is stored on disc and has to be read serially and distributed to all the nodes. Also the writing of results cannot yet be done entirely in parallel. Further details on the parallel architecture of the code can be found in Skålin et al. (1995).

The most CPU demanding part of the program is the chemistry module, because of the large number of chemical components and reactions. The chemical reactions have to be described for all the grid-cells and with a small time scales. However the chemistry is local and is therefore perfectly suited for parallelization. The deposition and wet scavenging processes have only vertical data dependencies and will therefore also parallelize effectively with the partitioning adopted in the program.

A typical run covering one year in a 159x133 grid will require less than four real time hours (128 CPU hours) on 32 processors. The typical relative CPU usage of the different part of the program are: Chemistry 60% , Advection 10%, Meteorology and input/output 10%, Synchronisation between nodes 10%, others 10%. For larger grids more processors are used; the model have been tested for up to 1024 CPUs and scales well.

A3 Derivation of 'missing' meteorological parameters

As noted in section 3 the EMEP model has to have systems for deriving parameters when missing, or can do without some meteorological fields. Two important cases are for 3-D precipitation and vertical wind-speed.

A3.1 3-D precipitation fields

When the precipitations are not available as a three dimensional field, they are derived from surface precipitations. The height of the precipitation release is derived either from cloud water, if available, or humidity if cloud water is not available. The height of the precipitation is then defined as the highest altitude above the lowest level, where the cloud water is larger than a threshold taken as 1.0×10^{-7} kg water per kg air (or when the relative humidity is larger 0.85 in case cloud water is not available). Precipitations are only defined in areas where surface precipitations occur. The intensity of the precipitation is assumed constant over all heights were they are non-zero.

A3.2 Vertical wind speed

When the vertical wind speed $\dot{\sigma}$ is not available, it is derived from the continuity equation (see also Travnikov et al. (2009)) using

$$(\dot{\sigma})_{k+\frac{1}{2}}(P_S - P_{top}) = \sigma_{k+\frac{1}{2}} \sum_{r=Surf}^{top} \nabla(\mathbf{V}_r \Delta P_r) - \sum_{r=k}^{top} \nabla(\mathbf{V}_r \Delta P_r) \quad (A7)$$

Use of this formula directly ensures that $(\dot{\sigma})_S = 0$ at surface since $\sigma_S = 1$, and $(\dot{\sigma})_{top} = 0$ at top since $\sigma_{top} = 0$.

A4 Emissions, additional information

Table A2. Vertical distribution of anthropogenic emissions: percentage of each SNAP emission sector allocated to the vertical layers of the EMEP model (given as heights of layers, in m, for a standard atmosphere).

No.	Sources	Height of Emission Layer (m)					
		0-92	92-184	184-324	324-522	522-781	781-1106
1	Combustion in energy and transformation industries			15	40	30	15
2	Non-industrial combustion plants	90	10				
3	Combustion in manufacturing industry	10	10	15	30	30	5
4	Production processes	90	10				
5	Extraction and distribution of fossil fuels and geothermal energy	90	10				
6	Solvents and other product use	100					
7	Road transport	100					
8	Other mobile sources and machinery	100					
9	Waste treatment and disposal	10	15	40	35		
10	Agriculture	100					

Table A3. Day^(a) and night factors applied to anthropogenic emissions

SNAP:	1	2	3	4	5	6	7	8 ^(b)	9	10
Day	1.0	1.2	1.2	1.5	1.0	1.5	1.5	1.2	1.0	1.4
Night	1.0	0.8	0.8	1.0	1.0	0.5	0.5	0.8	1.0	0.6

Notes: (a) Defined as between 7am and 6pm local time; (b) SNAP8 covers a range of non-road traffic sources, including shipping. Emissions from international shipping assumed constant over 24 h.

Table A4. Default speciation of VOC emissions: Percentage (by mass) of each emissions (SNAP) sector allocated to model species. Data derived from Passant (2002), see also Hayman et al. (2011).

SNAP	C2H6	NC4H10	C2H4	C3H6	C5H8	OXYL	CH3OH	C2H5OH	HCHO	CH3CHO	MEK	GLYOX	MGLYOX	UNREAC
1	12.559	14.836	2.406	4.376	0.000	9.479	0.000	0.000	55.691	0.034	0.620	0.000	0.000	0.000
2	12.589	39.790	8.174	10.767	0.000	18.632	0.000	3.912	5.586	0.207	0.089	0.000	0.000	0.255
3	4.996	35.610	9.044	2.089	0.000	18.323	0.561	3.034	24.134	0.059	1.347	0.000	0.000	0.805
4	2.652	34.519	5.458	4.257	0.142	13.380	1.176	31.414	0.077	0.978	1.608	0.000	0.000	4.337
5	17.842	79.895	0.018	1.569	0.008	0.505	0.000	0.000	0.078	0.000	0.000	0.000	0.000	0.085
6	0.444	44.052	0.244	0.678	0.008	17.904	6.101	16.416	0.011	0.000	9.965	0.000	0.000	4.176
7	4.832	36.698	6.796	10.896	0.000	35.051	0.000	0.000	2.700	2.606	0.421	0.000	0.000	0.000
8	3.775	47.416	6.636	10.608	0.000	24.676	0.000	0.000	3.115	3.261	0.235	0.146	0.117	0.014
9	25.718	36.778	5.237	1.830	1.153	7.881	0.427	2.439	16.060	0.000	0.093	0.000	0.000	2.383
10	0.000	0.000	0.000	0.000	0.000	0.000	0.000	0.000	0.000	0.000	0.000	0.000	0.000	100.000

Notes: For definition of model species (e.g. MEK, OXYL) see section 7, Table A5, except for non-reacting species here (UNREAC) which are excluded from the calculations.

Table A5. Default speciation of coarse (2.5–10 μ m) PM emissions: Percentage (by mass) of each emission (SNAP) sector allocated to organic matter (OM), elemental carbon (EC) and remaining coarse primary particulate matter (PPM_c).

SNAP	OM	EC ^(a)	PPM _c
1	1	5	94
2	50	20	30
3	5	10	85
4	5	5	90
5	5	5	90
6	10	40	50
7	40	30	30
8	45	45	10
9	40	30	30
10	40	20	40
11	70	0	30

(a) EC further split into 80% EC_{new.f}, 20% EC_{age.f}. If explicit wood-burning emissions available, a 50:50 split is assumed between EC_{new.f}, EC_{age.f}.

Table A6. Forest-specific biomass density and emission factors (leaf-level).

EMEP Code (Λ)	Species (λ)	Common name	Biomass density (D) gm^{-2}	Emission factors ($\mu\text{g g}^{-1}\text{h}^{-1}$)		
				Isoprene $\varepsilon_{\Lambda_c, iso}$	Monoterpenes $\varepsilon_{\Lambda_c, mtl}$	$\varepsilon_{\Lambda_c, mtp}$
CF	Abies alba	Silver Fir	1200	0	0	1
CF	Abies bori.	Bulgarian Fir	1200	10	0	3
CF	Abies	other Fir	1200	0	0	3
DF	Acer		320	0	2	0
DF	Alnus glutinosa	Common Alder	320	0.2	3	0
DF	Alnus	other Alder	320	0	1.5	0
BF	Arbutus		300	0.1	0.1	0
DF	Betula	Birch		320	0	0
NF	Buxus Semi.	Common box	320	10	0	0.2
DF	Carpinus bet.	European Hornbeam	320	0	0	0.7
DF	Carpinus	other Hornbeam	320	0	1	0.5
DF	Castanea	Chestnut - all	320	0	10	0
NF	Cedrus	Cedar	700	0	0	0.7
DF	Cercis sil.	Judas tree	320	0	0	0
NF	Ceratonia silq	Carob tree	320	0	0	0
DF	Corylus avel.	Hazel tree	320	0	0	0
NF	Cupressus	Cypress	700	0.1	0	0.7
NF	Erica arbor.	Tree Heath	100	10	0	3
NF	Erica	other Erica	150	0	0	0
NF	Eucalyptus	Eucalyptus	400	35	0	3
DF	Fagus	Beech	320	0	10	0

Notes: See section 6.6 for explanation of rates and algorithms.

Table A6. cont.

Λ	λ		D	$\varepsilon_{\Lambda_c, iso}$	$\varepsilon_{\Lambda_c, mtl}$	$\varepsilon_{\Lambda_c, mtp}$
DF	Fraxinus	Ash (all)	320	0	0	0
NF	Ilex aqu.	Holly	320	0	0	0
BF	Juglans	Walnut	320	0	0	1
NF	Juniperus	Juniper	700	0	0	1
DF	Larix kaemp.		300	0	0	8
DF	Larix	Larch (other)	300	0	0	5
NF	Laurus nobilis	Laurel	500	0	0	0
DF	malus domestica	Apple	320	0	0	0
NF	Olea	Olive	200	0	0.2	0
DF	Ostrya Carp.	Hop Hornbeam	320	0	0	0
NF	Philyrea latifolia	Green Olive	300	0	0.4	0.1
CF	Picea abies	Norway spruce	1400	1	0.5	1
CF	Picea sitch.	Sitka spruce	1400	5	0	3
CF	Picea	Other spruce	1400	1	0.5	1
NF	Pinus pinaster	Maritime pine	700	0	0	1.5
NF	Pinus pinea	Stone pine	700	0	4	2
CF	Pinus sylvestris	Scots pine	700	0.1	1	2
CF	Pinus uncinata	Mountain pine	700	0.1	0	3
NF	Pinus radiata	Monterey pine	700	0	1	1
CF	Pinus - other	Other pine	700	0	0	3
BF	Pistacia lent.		320	0	0	0.7
BF	Pistacia tere.		320	0	0.5	0
DF	Platanus orientali	Oriental plane	320	50	0	3
DF	Populus alba		320	60	1	0
DF	Populus tremula		320	45	3	0
DF	Populus	Other Poplar	320	45	1	0
DF	Prunus		300	0	0.2	0
CF	Pseudotsuga menz.	Douglas Fir	1000	1	0	3
DF	Pyrus comm.	European pear	320	0	0	0

Table A6. cont.

Λ	λ		D	$\varepsilon_{\Lambda_c, iso}$	$\varepsilon_{\Lambda_c, mtI}$	$\varepsilon_{\Lambda_c, mtP}$
DF	Quercus cerr.	Turkey oak	320	0.1	1	0.5
BF	Quercus cocce.	Kermes oak	320	0.1	10	0
DF	Quercus fagi.	Portugese oak	320	100	0.5	0
DF	Quercus frai.	Hungarian(Italian) oak	320	100	0	0
BF	Quercus fruc.		320	0.1	20	0
BF	Quercus ilex.	Holm (Holly) Oak	500	0.1	30	0
DF	Quercus macr.	Caucasian(Persian)	320	0.2	0	0.5
DF	Quercus petr.	Sessile oak	320	45	0.5	0
DF	Quercus pube.	Downy oak	320	80	0.2	0
DF	Quercus pyre.	Pyerenean oak	320	60	0.5	0
DF	Quercus robu.	Pendunculate(English)	320	80	0.2	0.2
BF	Quercus rotu.		320	0.2	15	0
DF	Quercus rubra	N. Red Oak	320	60	1	0
BF	Quercus sube.	Cork oak	500	0.2	20	0
BF	Quercus troj.	Macedonian oak	320	0.2	0.2	0
DF	Robinia pseu.	Locust	320	20	3	0
DF	Salix	Willow	150	20	0	1
DF	Sorbus	Whitebeam	320	0	0	0
DF	Taxus baccata	Yew	320	0	0	0
CF	Thuja sp.		320	0	0	0.5
DF	Tilia sp.	Lime/Linden	320	0	0	0
CF	Tsuga sp.	Hemlock	320	0.1	0	1.5
DF	Ulmus sp.	Elm	320	0.1	0	0.1
DF	Other broadleaf		320	5	0	0.2
CF	Other coniferous		500	1	1	2

A5 Default chemical mechanism, EmChem09

We give below the gas and inorganic particle phase chemical mechanism. (For comments on secondary organic aerosol, see Sect. 7.9.)

Table A7. Listing of non-advected (short-lived) species used in default EmChem09 chemical scheme.

Model species	Formula
OD	O
OP	O
OH	OH
HO2	HO2
CH3O2	CH3O2
C2H5O2	C2H5O2
SECC4H9O2	secC4H9O2
ISRO2	HOC5H8O2
ETRO2	CH2O2CH2OH
PRRO2	CH3CHO2CH2OH
OXYO2	C8H11O3O2
MEKO2	CH3COCHO2CH3
MALO2	CH3COCH(OH)CH(O2)CHO
MVKO2	HOCH2CH(OO)C(CH3)=O
MACRO2	O=CHC(O2)(CH3)CH2OH
MACO3	CH2C(CH3)C(=O)O2

Table A8. Listing of advected core species used in default EmChem09 chemical scheme.

Model species	Formula	DRY [†]	WET [†]
O3	O3	O3	
NO	NO		
NO2	NO2	NO2	
PAN	CH3COO2NO2	PAN	
MPAN	CH2CH(CH3)C(=O)O2NO2	PAN	
NO3	NO3		
N2O5	N2O5		
ISONO3	NO3C5H8O		
HNO3	HNO3	HNO3	HNO3
HONO	HONO	HNO2	HNO3
H2	H2		
CO	CO		
CH4	CH4		
SO2	SO2	SO2	SO2
SO4	SO4	PMfS	SO4
NH3	NH3	NH3	NH3
NO3 _f	NO3	PMfN	PMf
NO3 _c	NO3	PMc	PMc
NH4 _f	NH4	PMfN	PMf
CH3COO2	CH3COO2		
MACR	CH2=CCH3CHO		
ISNI	generic		
ISNIR	generic		
GLYOX	HCOHCO		
MGLYOX	CH3COCHO		
MAL	CH3COCH=CHCHO	ALD	
MEK	CH3COC2H5		
MVK	CH3C(=O)CH=CH2		
HCHO	HCHO	HCHO	HCHO

Table gives: Spec – species name as used in code, Formula – chemical formula when needed by GenChem (sometimes omitted), DRY – species from which dry-deposition rates calculated, WET – species from which wet-deposition rates calculated.

[†] Notation for gaseous compounds relates to *Wesely, 1989*, although methodology differs. PMfS, PMfN, PMc are particle deposition rates for sulphate, nitrogen-containing and coarse aerosols. Suffix *_f*, *_c* refer to fine and coarse mode aerosol species.

The Table omits the species involved in the SOA mechanism, since these vary very much with mechanism, and also do not affect the core chemistry.

Table A8. cont.

Model species	Formula	DRY	WET
CH3CHO	CH3CHO	ALD	
C2H6	C2H6		
NC4H10	nC4H10		
C2H4	C2H4		
C3H6	C3H6		
OXYL	oC6H4(CH3)CH3		
C5H8	CH2=HCC=CH2CH3		
CH3O2H	CH3O2H	ROOH	
C2H5OOH	C2H5OOH	ROOH	
BURO2H	secC4H9O2H		
ETRO2H	CH2O2HCH2OH		
PRRO2H	CH3CHO2HCH2OH		
OXYO2H	C8H11O3O2H		
MEKO2H	CH3COCHO2HCH3		
MALO2H	CH3COCHOHCHO2CHO		
MVKO2H	HOCH2CH(O2H)C(CH3)=O		
MACROOH	O=CHC(CH3)(OOH)CH2OH		
MACO3H	CH2=C(CH3)C(=O)OOH		
MACO2H	CH2=C(CH3)C(=O)OH		
ISRO2H	HOC5H8O2H		
H2O2	H2O2	SO2	H2O2
CH3COO2H	CH3COO2H		
ISONO3H	NO3C5H8O2H		
ISNIRH	generic		
CH3OH	CH3OH		
C2H5OH	C2H5OH		
ACETOL	CH3COCH2OH	ALD	

Table A9. Listing of some optional, inert and tracer species

Model species	Formula	DRY [†]	WET [†]	Comments
APINENE	C10H16			Used if SOA scheme
ECnew_f		PMfS	PMecf	Fresh (hydrophobic) EC
ECage_f		PMfS	PMf	Aged (mixed, and hydrophillic) EC
SeaSalt_f		PMfS	PMssf	
SeaSalt_c		PMc	PMssc	
Dust_f		PMfS	PMf	
Dust_c		PMc	PMc	
PPM_f		PMfS	PMf	primary particulate matter, fine-mode (excluding OM, EC)
PPM_c		PMc	PMc	
PPM25_FIRE		PMfS	PMf	Fire tracer
CO_FIRE	CO			Fire tracer
Rn222				Radon isotope tracer
Pb210		PMfS	PMf	Product from radon decay

Notes: Suffix _f, _c refer to fine and coarse mode aerosol species.

Table A10. Default Chemical Mechanism of EMEP model, EmChem09. For Notes, see end of Table

N	Rate coefficient	Reaction
<i>Inorganic chemistry</i>		
IN-1	$(6.0 \times 10^{-34} \text{ O}_2 + 5.6 \times 10^{-34} \text{ N}_2) \times \text{O}_2 \times \exp(-2.6 \ln(T/300))$	$\text{OP} + \text{O}_2 + \text{M} \Rightarrow \text{O}_3$
IN-2	$1.8 \times 10^{-11} \exp(107/T) \times \text{N}_2$	$\text{OD} + \text{N}_2 \Rightarrow \text{OP}$
IN-3	$3.2 \times 10^{-11} \exp(67/T) \times \text{O}_2$	$\text{OD} + \text{O}_2 \Rightarrow \text{OP}$
IN-4	$2.2 \times 10^{-10} \text{ H}_2\text{O}$	$\text{OD} + \text{H}_2\text{O} \Rightarrow 2. \text{OH}$
IN-5	$1.4 \times 10^{-12} \exp(-1310/T)$	$\text{O}_3 + \text{NO} \Rightarrow \text{NO}_2 + \text{O}_2$
IN-6	$1.4 \times 10^{-13} \exp(-2470/T)$	$\text{O}_3 + \text{NO}_2 \Rightarrow \text{NO}_3 + \text{O}_2$
IN-7	$1.7 \times 10^{-12} \exp(-940/T)$	$\text{O}_3 + \text{OH} \Rightarrow \text{HO}_2 + \text{O}_2$
IN-8	$2.03 \times 10^{-16} \times \exp(-4.57 \ln(300/T)) \exp(693/T)$	$\text{O}_3 + \text{HO}_2 \Rightarrow \text{OH} + 2 \text{O}_2$
IN-9	$1.8 \times 10^{-11} \exp(110/T)$	$\text{NO} + \text{NO}_3 \Rightarrow \text{NO}_2 + \text{NO}_2$
IN-10	$3.6 \times 10^{-12} \exp(270/T)$	$\text{NO} + \text{HO}_2 \Rightarrow \text{NO}_2 + \text{OH}$
IN-11	$4.5 \times 10^{-14} \exp(-1260/T)$	$\text{NO}_2 + \text{NO}_3 \Rightarrow \text{NO} + \text{NO}_2$
IN-12	$4.8 \times 10^{-11} \exp(250/T)$	$\text{OH} + \text{HO}_2 \Rightarrow \text{H}_2\text{O} + \text{O}_2$
IN-13	$2.9 \times 10^{-12} \exp(-160/T)$	$\text{OH} + \text{H}_2\text{O}_2 \Rightarrow \text{HO}_2 + \text{H}_2\text{O}$
IN-14	$7.7 \times 10^{-12} \exp(-2100/T)$	$\text{OH} + \text{H}_2 \Rightarrow \text{HO}_2 + \text{H}_2\text{O}$
IN-15	$k_{\text{OH}+\text{HNO}_3}$	$\text{OH} + \text{HNO}_3 \Rightarrow \text{NO}_3 + \text{H}_2\text{O}$
IN-16	$k_{\text{HO}_2+\text{HO}_2}$	$\text{HO}_2 + \text{HO}_2 \Rightarrow \text{H}_2\text{O}_2$
IN-17	$2.5 \times 10^{-12} \exp(-260/T)$	$\text{OH} + \text{HONO} \Rightarrow \text{NO}_2$
IN-18	$k_{\text{N}_2\text{O}_5}$	$\text{N}_2\text{O}_5 \Rightarrow 2. \text{HNO}_3$
IN-19	k_{aero}	$\text{HNO}_3 \Rightarrow \text{NO}_3\text{c}$
IN-20	$kt_{\text{NO}+\text{OP}}$	$\text{OP} + \text{NO} + \text{M} \Rightarrow \text{NO}_2$
IN-21	$kt_{\text{NO}_2+\text{NO}_3}$	$\text{NO}_2 + \text{NO}_3 \Rightarrow \text{N}_2\text{O}_5$
IN-22	$kt_{\text{N}_2\text{O}_5}$	$\text{N}_2\text{O}_5 \Rightarrow \text{NO}_2 + \text{NO}_3$
IN-23	$kt_{\text{NO}_2+\text{OH}}$	$\text{NO}_2 + \text{OH} + \text{M} \Rightarrow \text{HNO}_3$
IN-24	$kt_{\text{OH}+\text{NO}}$	$\text{OH} + \text{NO} \Rightarrow \text{HONO}$
<i>Sulphate (inc. in-cloud) formation</i>		
cl-OH	(a)	$\text{OH} + \text{SO}_2 \Rightarrow \text{HO}_2 + \text{SO}_4$
cl-1	(a)	$\text{SO}_2 + \text{H}_2\text{O}_2 \Rightarrow \text{SO}_4$
cl-2	(a)	$\text{SO}_2 + \text{O}_3 \Rightarrow \text{SO}_4$
cl-3	(a)	$\text{SO}_2 + \text{Fe} \Rightarrow \text{SO}_4$

Table A10. cont.

N	Rate coefficient	Reaction
<i>Methane chemistry</i>		
MA-1	$1.85 \times 10^{-20} \times \exp(2.82 \ln(T)) \times \exp(-987/T)$	$\text{OH} + \text{CH}_4 \Rightarrow \text{CH}_3\text{O}_2$
MA-2	$1.44 \times 10^{-13} + 3.43 \times 10^{-33} \text{ M}$	$\text{OH} + \text{CO} \Rightarrow \text{HO}_2$
MA-3	$2.3 \times 10^{-12} \exp(360/T)$	$\text{CH}_3\text{O}_2 + \text{NO} \Rightarrow \text{HCHO} + \text{HO}_2 + \text{NO}_2$
MA-4	$7.4 \times 10^{-13} \exp(-520/T)$	$\text{CH}_3\text{O}_2 + \text{CH}_3\text{O}_2 \Rightarrow 2. \text{HCHO} + 2. \text{HO}_2$
MA-5	$1.03 \times 10^{-13} \exp(365/T)$ $7.4 \times 10^{-13} \exp(-520/T)$	$\text{CH}_3\text{O}_2 + \text{CH}_3\text{O}_2 \Rightarrow \text{CH}_3\text{OH} + \text{HCHO}$
MA-6	$6.38 \times 10^{-18} \exp(144/T) \times T^2$	$\text{OH} + \text{CH}_3\text{OH} \Rightarrow \text{HO}_2 + \text{HCHO} + \text{H}_2\text{O}$
MA-7	$3.8 \times 10^{-13} \exp(780/T)$	$\text{HO}_2 + \text{CH}_3\text{O}_2 \Rightarrow 0.9 \text{CH}_3\text{O}_2\text{H} + 0.1 \text{HCHO}$
MA-8	$5.3 \times 10^{-12} \exp(190/T)$	$\text{CH}_3\text{O}_2\text{H} + \text{OH} \Rightarrow 0.4 \text{HCHO} + 0.4 \text{OH} + 0.6 \text{CH}_3\text{O}_2 + 0.6 \text{H}_2\text{O}$
<i>Ethane and ethanol chemistry</i>		
EA-1	$1.25 \times 10^{-17} \times T^2 \times \exp(615/T)$	$\text{OH} + \text{HCHO} \Rightarrow \text{CO} + \text{HO}_2 + \text{H}_2\text{O}$
EA-2	$2.0 \times 10^{-12} \exp(-2440/T)$	$\text{NO}_3 + \text{HCHO} \Rightarrow \text{HNO}_3 + \text{CO} + \text{HO}_2$
EA-3	$6.9 \times 10^{-12} \exp(-1000/T)$	$\text{OH} + \text{C}_2\text{H}_6 \Rightarrow \text{C}_2\text{H}_5\text{O}_2 + \text{H}_2\text{O}$
EA-4	$6.9 \times 10^{-12} \exp(-1000/T)$	$[\text{OH}] + \text{C}_2\text{H}_6 \Rightarrow$
EA-5	$2.55 \times 10^{-12} \exp(380/T)$	$\text{C}_2\text{H}_5\text{O}_2 + \text{NO} \Rightarrow \text{HO}_2 + \text{CH}_3\text{CHO} + \text{NO}_2$
EA-6	$3.8 \times 10^{-13} \exp(900/T)$	$\text{C}_2\text{H}_5\text{O}_2 + \text{HO}_2 \Rightarrow \text{C}_2\text{H}_5\text{OOH}$
EA-7	8.01×10^{-12}	$\text{C}_2\text{H}_5\text{OOH} + \text{OH} \Rightarrow \text{CH}_3\text{CHO} + \text{OH}$
EA-8	$k_{\text{OH}+\text{ROOH}}$	$\text{C}_2\text{H}_5\text{OOH} + \text{OH} \Rightarrow \text{C}_2\text{H}_5\text{O}_2$
EA-9	$4.4 \times 10^{-12} \exp(365/T)$	$\text{OH} + \text{CH}_3\text{CHO} \Rightarrow 0.95 \text{CH}_3\text{COO}_2 + 0.05 \text{CH}_3\text{O}_2 + 0.05 \text{CO}$
EA-10	kt_{panf}	$\text{CH}_3\text{COO}_2 + \text{NO}_2 + \text{M} \Rightarrow \text{PAN}$
EA-11	kt_{panb}	$\text{PAN} + \text{M} \Rightarrow \text{CH}_3\text{COO}_2 + \text{NO}_2$
EA-12	$7.5 \times 10^{-12} \exp(290/T)$	$\text{CH}_3\text{COO}_2 + \text{NO} \Rightarrow \text{NO}_2 + \text{CH}_3\text{O}_2 + \text{CO}_2$
EA-13	$2.0 \times 10^{-12} \exp(500/T)$	$\text{CH}_3\text{O}_2 + \text{CH}_3\text{COO}_2 \Rightarrow 0.9 \text{HO}_2 + \text{HCHO} + 0.9 \text{CH}_3\text{O}_2 + 0.1 \text{CH}_3\text{COOH}$
EA-14	$2.9 \times 10^{-12} \exp(500/T)$	$\text{CH}_3\text{COO}_2 + \text{CH}_3\text{COO}_2 \Rightarrow \text{CH}_3\text{O}_2 + \text{CH}_3\text{O}_2$
EA-15	$5.2 \times 10^{-13} \exp(980/T)$	$\text{CH}_3\text{COO}_2 + \text{HO}_2 \Rightarrow 0.41 \text{CH}_3\text{COO}_2\text{H} + 0.15 \text{O}_3 + 0.44 \text{OH} + 0.44 \text{CH}_3\text{O}_2 + 0.15 \text{CH}_3\text{COOH}$
EA-16	$1.9 \times 10^{-12} \exp(190/T)$	$\text{CH}_3\text{COO}_2\text{H} + \text{OH} \Rightarrow \text{CH}_3\text{COO}_2$
EA-17	$6.7 \times 10^{-18} \exp(511/T) \times T^2$	$\text{OH} + \text{C}_2\text{H}_5\text{OH} \Rightarrow \text{CH}_3\text{CHO} + \text{HO}_2$

Table A10. cont.

N	Rate coefficient	Reaction
<i>n-butane chemistry</i>		
NB-1	$2.03 \times 10^{-17} \exp(78/T) T^2$	$\text{OH} + \text{NC4H10} \Rightarrow \text{SECC4H9O2}$
NB-2	$k_{\text{NO}+\text{RO2}}$	$\text{NO} + \text{SECC4H9O2} \Rightarrow \text{NO2} + 0.65 \text{HO2} + 0.65 \text{MEK} + 0.35 \text{CH3CHO} + 0.35 \text{C2H5O2}$
NB-3	$0.625 \times k_{\text{HO2}+\text{RO2}}$	$\text{SECC4H9O2} + \text{HO2} \Rightarrow \text{BURO2H}$
NB-4	$2.53 \times 10^{-18} \exp(503/T) T^2$	$\text{OH} + \text{MEK} \Rightarrow \text{MEKO2}$
NB-5	$k_{\text{NO}+\text{RO2}}$	$\text{MEKO2} + \text{NO} \Rightarrow \text{NO2} + \text{CH3COO2} + \text{CH3CHO}$
NB-6	$0.625 \times k_{\text{HO2}+\text{RO2}}$	$\text{MEKO2} + \text{HO2} \Rightarrow \text{MEKO2H}$
NB-7	$1.9 \times 10^{-12} \exp(190/T)$	$\text{MEKO2H} + \text{OH} \Rightarrow \text{MEKO2}$
NB-8	$k_{\text{OH}+\text{ROOH}}$	$\text{BURO2H} + \text{OH} \Rightarrow \text{SECC4H9O2}$
NB-9	2.15×10^{-11}	$\text{BURO2H} + \text{OH} \Rightarrow \text{OH} + \text{MEK}$
<i>Ethene chemistry</i>		
EE-1	$kt_{\text{OH}+\text{C2H4}}$	$\text{C2H4} + \text{OH} + \text{M} \Rightarrow \text{ETRO2}$
EE-2	$k_{\text{NO}+\text{RO2}}$	$\text{ETRO2} + \text{NO} \Rightarrow \text{NO2} + 2. \text{HCHO} + \text{HO2}$
EE-3	1.2×10^{-11}	$\text{ETRO2} + \text{HO2} \Rightarrow \text{ETRO2H}$
EE-4	1.38×10^{-11}	$\text{ETRO2H} + \text{OH} \Rightarrow \text{CH3CHO} + \text{OH}$
EE-5	$k_{\text{OH}+\text{ROOH}}$	$\text{ETRO2H} + \text{OH} \Rightarrow \text{ETRO2}$
EE-6	$9.1 \times 10^{-15} \exp(-2580/T)$	$\text{C2H4} + \text{O3} \Rightarrow 1.14 \text{HCHO} + 0.63 \text{CO} + 0.13 \text{HO2} + 0.13 \text{OH} + 0.14 \text{H2O2} + 0.23 \text{HCOOH}$
<i>Propene chemistry</i>		
PE-1	$5.5 \times 10^{-15} \exp(-1880/T)$	$\text{O3} + \text{C3H6} \Rightarrow 0.545 \text{HCHO} + 0.545 \text{CH3CHO} + 0.56 \text{CO} + 0.36 \text{OH} + 0.28 \text{HO2} + 0.09 \text{H2O2} + 0.1 \text{CH4} + 0.28 \text{CH3O2} + 0.075 \text{HCOOH} + 0.075 \text{CH3COOH}$
PE-2	$kt_{\text{OH}+\text{C3H6}}$	$\text{OH} + \text{C3H6} + \text{M} \Rightarrow \text{PRRO2}$
PE-3	$k_{\text{NO}+\text{RO2}}$	$\text{NO} + \text{PRRO2} \Rightarrow \text{NO2} + \text{CH3CHO} + \text{HCHO} + \text{HO2}$
PE-4	$0.52 \times k_{\text{HO2}+\text{RO2}}$	$\text{PRRO2} + \text{HO2} \Rightarrow \text{PRRO2H}$
PE-5	2.44×10^{-11}	$\text{PRRO2H} + \text{OH} \Rightarrow \text{ACETOL} + \text{OH}$
PE-6	$k_{\text{OH}+\text{ROOH}}$	$\text{PRRO2H} + \text{OH} \Rightarrow \text{PRRO2}$

Table A10. cont.

N	Rate coefficient	Reaction
<i>o-xylene chemistry</i>		
OX-1	1.36×10^{-11}	OXYL + OH \Rightarrow OXYO2
OX-2	k_{NO+RO2}	OXYO2 + NO \Rightarrow NO2 + MGLYOX + MAL + HO2
OX-3	$0.859 \times k_{HO2+RO2}$	OXYO2 + HO2 \Rightarrow OXYO2H
OX-4	4.2×10^{-11}	OXYO2H + OH \Rightarrow OXYO2
OX-5	5.58×10^{-11}	MAL + OH \Rightarrow MALO2
OX-6	k_{NO+RO2}	MALO2 + NO \Rightarrow NO2 + HO2 + MGLYOX + GLYOX
OX-7	$0.706 \times k_{HO2+RO2}$	MALO2 + HO2 \Rightarrow MALO2H
OX-8	$1.9 \times 10^{-12} \exp(190/T)$	MALO2H + OH \Rightarrow MALO2
OX-9	$6.6 \times 10^{-18} \exp(820/T) \times T^2$	OH + GLYOX \Rightarrow HO2 + 2 CO
<i>Isoprene chemistry</i>		
IS-1	$1.03 \times 10^{-14} \exp(-1995/T)$	C5H8 + O3 \Rightarrow 0.67 MACR + 0.26 MVK + 0.3 OP + 0.55 OH + 0.07 C3H6 + 0.8 HCHO + 0.06 HO2 + 0.05 CO
IS-2	$2.7 \times 10^{-11} \exp(390/T)$	C5H8 + OH \Rightarrow ISRO2
IS-3	k_{NO+RO2}	ISRO2 + NO \Rightarrow 0.32 MACR + 0.42 MVK + 0.74 HCHO + 0.14 ISNI + 0.12 ISRO2 + 0.78 HO2 + 0.86 NO2
IS-4	$0.706 \times k_{HO2+RO2}$	ISRO2 + HO2 \Rightarrow ISRO2H
IS-5	$2.6 \times 10^{-12} \exp(610/T)$	MVK + OH \Rightarrow MVKO2
IS-6	k_{NO+RO2}	MVKO2 + NO \Rightarrow 0.684 CH3CHO + 0.684 CH3COO2 + 0.266 MGLYOX + 0.266 HCHO + 0.05 ISNI + 0.95 NO2 + 0.95 HO2
IS-7	7.5×10^{-11}	ISRO2H + OH \Rightarrow OH + ISRO2
IS-8	$1.36 \times 10^{-15} \exp(-2112/T)$	MACR + O3 \Rightarrow 0.59 MGLYOX + 0.41 HO2 + 0.82 CO + 0.82 OH + 0.534 HCHO + 0.124 H2O2 + 0.41 CH3COO2 + 0.056 HCOOH
IS-9	$8.0 \times 10^{-12} \exp(380/T)$	MACR + OH \Rightarrow 0.5 MACRO2 + 0.5 MACO3
IS-10	kt_{panf}	MACO3 + NO2 \Rightarrow MPAN
IS-11	kt_{panb}	MPAN \Rightarrow MACO3 + NO2
IS-12	$7.6 \times 10^{-12} \exp(180/T)$	MACRO2 + NO \Rightarrow 0.95 HO2 + 0.95 CO + 0.95 ACETOL + 0.05 ISNI + 0.95 NO2
IS-13	2.5×10^{-12}	MACRO2 + NO3 \Rightarrow NO2 + ACETOL + HCHO + HO2
IS-14	$0.625 \times k_{HO2+RO2}$	MACRO2 + HO2 \Rightarrow MACROOH + O2
IS-15	2.82×10^{-11}	MACROOH + OH \Rightarrow MACRO2
IS-16	$1.6 \times 10^{-12} \exp(305/T)$	ACETOL + OH \Rightarrow MGLYOX + HO2
IS-17	$8.7 \times 10^{-12} \exp(290/T)$	MACO3 + NO \Rightarrow CH3COO2 + HCHO + NO2

Table A10. cont.

N	Rate coefficient	Reaction
<i>Isoprene cont.</i>		
IS-18	$8.5 \times 10^{-16} \exp(-1520/T)$	MVK + O3 \Rightarrow 0.82 MGlyox + 0.8 HCHO + 0.2 OP + 0.05 CO + 0.06 HO2 + 0.04 CH3CHO + 0.08 OH
IS-19	5.96×10^{-11}	ISNI + OH \Rightarrow ISNIR
IS-20	k_{NO+RO2}	ISNIR + NO \Rightarrow 0.05 ISNI + 0.05 HO2 + 1.9 NO2 + 0.95 CH3CHO + 0.95 ACETOL
IS-21	$3.15 \times 10^{-12} \exp(-450/T)$	C5H8 + NO3 \Rightarrow ISONO3
IS-22	k_{NO+RO2}	ISONO3 + NO \Rightarrow 1.1 NO2 + 0.8 HO2 + 0.85 ISNI + 0.1 MACR + 0.15 HCHO + 0.05 MVK
IS-23	$0.706 \times k_{HO2+RO2}$	ISONO3 + HO2 \Rightarrow ISONO3H
IS-24	$0.625 \times k_{HO2+RO2}$	MVKO2 + HO2 \Rightarrow MVKO2H
IS-25	$4.3 \times 10^{-13} \exp(1040/T)$	MACO3 + HO2 \Rightarrow 0.71 MACO3H + 0.29 MACO2H + 0.29 O3
IS-26	1.87×10^{-11}	MACO3H + OH \Rightarrow MACO3
IS-27	1.51×10^{-11}	MACO2H + OH \Rightarrow CH3COO2 + HCHO
IS-28	$0.706 \times k_{HO2+RO2}$	ISNIR + HO2 \Rightarrow ISNIRH
IS-29	2.0×10^{-11}	ISONO3H + OH \Rightarrow ISONO3
IS-30	2.2×10^{-11}	MVKO2H + OH \Rightarrow MVKO2
IS-31	3.7×10^{-11}	ISNIRH + OH \Rightarrow ISNIR
IS-32	2.9×10^{-11}	MPAN + OH \Rightarrow ACETOL + CO + NO2
<i>Miscellaneous</i>		
MS-1	2.1E-6	RN222 \Rightarrow PB210
MS-2	1.0E-12 \times H2O	PB210 \Rightarrow aerosol sink
MS-3	1.0E-5	H2O2 \Rightarrow aerosol sink
MS-4	1.0E-5	CH3O2H \Rightarrow aerosol sink
MS-5	k_{ECage}	ECnew_f \Rightarrow ECage_f

Notes. T is temperature, M is third body; Reaction coefficients are in units of s^{-1} for unimolecular reactions, $cm^3 \text{ molecule}^{-1} s^{-1}$ for bimolecular reactions, and $cm^6 \text{ molecule}^{-2} s^{-2}$ for termolecular reactions. Reaction steps labelled as "Immediate" are given for clarity only. Rate-coefficients labelled with *kt* are given as Troe expressions in Table A11, and coefficients labelled with *k* are given in Table A12. (a) The 'cl' rates for sulphate formation involve cloud-water calculations and are discussed in sections 7.5-7.6;

Table A11. Rate-constants for 3-body reactions using the Troe expression^(a) The reaction rates are calculated as: $k = \frac{k_0 k_\infty}{k_0 + k_\infty} F$, with the broadening factor F calculated using the approximate expression: $\log_{10} F \cong \frac{\log_{10} F_c}{1 + [\log_{10} (k_0/k_\infty)/N]^2}$ where $N = [0.75 - 1.27 \log_{10} F_c]$ The first column (Rate coeff.) refers to the notation in

Table A10.

Rate coeff.	$k_0/[M]$	k_∞	F_c
kt_{NO+OP}	$1.0 \times 10^{-31} (300/T)^{1.6}$	$3.0 \times 10^{-11} (300/T)^{-0.3}$	0.85
$kt_{NO2+NO3}$	$3.6 \times 10^{-30} (300/T)^{4.1}$	$1.9 \times 10^{-12} (300/T)^{-0.2}$	0.35
kt_{N2O5}	$1.3 \times 10^{-3} (300/T)^{3.5} e^{(-11000/T)}$	$9.70 \times 10^{14} (300/T)^{-0.1} e^{(-11080/T)}$	0.35
kt_{NO2+OH}	$3.3e \times 10^{30} (300/T)^{3.0}$	4.1×10^{-11}	0.40
kt_{OH+NO}	$7.4 \times 10^{-31} (300/T)^{2.4}$	$3.3 \times 10^{-11} (300/T)^{0.3}$	$e^{(-T/1420)}$
$kt_{OH+C2H4}$	$8.6 \times 10^{-29} (300/T)^{3.1}$	$9.0 \times 10^{-12} (300/T)^{0.85}$	0.48
kt_{NO+OP}	$1.0 \times 10^{-31} (300/T)^{1.6}$	$3.0 \times 10^{-11} (300/T)^{-0.3}$	0.85
$kt_{OH+C3H6}$	$8.0 \times 10^{-27} (300/T)^{3.5}$	$3.0 \times 10^{-11} \exp(300/T)$	0.5
kt_{panf}	$2.7 \times 10^{-28} (300/T)^{7.1}$	$1.2 \times 10^{-11} (300/T)^{0.9}$	0.3
kt_{panb}	$4.9 \times 10^{-3} (300/T)^{-12100}$	$5.4 \times 10^{16} \exp(-13830/T)$	0.3

(a) For form of Troe expressions, see eg Atkinson et al. (2006).

Table A12. Other rate coefficients

No.	rate	Comments
$k_{OH+HNO3}$	$= K_1 + (K_3[M]) / (1.0 + (K_3[M])/K_4)$, where $K_1 = 2.4 \times 10^{-14} \exp(460/T)$, $K_2 = 6.5 \times 10^{-34} \exp(1335/T)$, $K_3 = 2.7 \times 10^{-17} \exp(2199/T)$	
$k_{HO2+HO2}$	$= F_{H2O} \times 2.2 \times 10^{-13} \exp(600/T) + F_{H2O} \times 1.9 \times 10^{-33} \exp(980/T) \times M$, where $F_{H2O} = 1.0 + 1.4 \times 10^{-21} \exp(2200/T) [H2O]$	
$k_{OH+ROOH}$	$= 1.9 \times 10^{-12} \exp(190/T)$	
$k_{HO2+RO2}$	$= 2.91 \times 10^{-13} \exp(1300/T)$	
k_{NO+RO2}	$= 2.54 \times 10^{-12} \exp(360/T)$	
k_{aero}	$= 1.0 \times 10^{-5}$ when RH>90%, else 5.0×10^{-6}	
$k_{ECage} \text{ (day)}$	$= 3.3 \times 10^{-6}$ for lowest 3 layers (<300m approx) $= 1.4 \times 10^{-4}$ for upper layers (>300m approx)	Tsyro et al. (2007)
$k_{ECage} \text{ (night)}$	$= 1.0 \times 10^{-5}$ for lowest 3 layers (<300m approx)	

Table A13. Photolysis reactions. For some reactions, rates are taken from given surrogate species, scaled if necessary

N	Reaction
J-O3A	$O_3 \Rightarrow OP$
J-O3B	$O_3 \Rightarrow OD$
J-NO2	$NO_2 \Rightarrow OP + NO$
J-H2O2	$H_2O_2 \Rightarrow 2 OH$
J-HNO3	$HNO_3 \Rightarrow NO_2 + OH$
J-HCHOA	$HCHO \Rightarrow CO + 2 HO_2$
J-HCHOB	$HCHO \Rightarrow CO + H_2$
J-CH3CHO	$CH_3CHO \Rightarrow CH_3O_2 + HO_2 + CO$
J-NO3	$NO_3 \Rightarrow NO_2 + OP$
J-CH3O2H	$CH_3O_2H \Rightarrow HCHO + OH + HO_2$
J-GLYOX	$GLYOX \Rightarrow 1.9 CO + 0.1 HCHO + 0.5 HO_2$
J-RCOHCO	$MGLYOX \Rightarrow CH_3COO_2 + CO + HO_2$
J-CH3O2H	$C_2H_5OOH \Rightarrow HO_2 + CH_3CHO + OH$
J-CH3O2H	$ETRO_2H \Rightarrow HO_2 + OH + 1.56 HCHO + 0.22 CH_3CHO$
J-CH3O2H	$BURO_2H \Rightarrow OH + 0.65 HO_2 + 0.65 MEK + 0.35 CH_3CHO + 0.35 C_2H_5O_2$
J-CH3O2H	$PRRO_2H \Rightarrow CH_3CHO + HCHO + HO_2$
J-CH3O2H	$MEKO_2H \Rightarrow CH_3CHO + CH_3COO_2 + OH$
J-CH3COX	$MEK \Rightarrow CH_3COO_2 + C_2H_5O_2$
J-CH3O2H	$CH_3COO_2H \Rightarrow CH_3O_2 + OH$
J-CH3O2H	$OXYO_2H \Rightarrow OH + MGLYOX + MAL + HO_2$
J-CH3O2H	$MALO_2H \Rightarrow OH + HO_2 + MGLYOX + GLYOX$
0.222 J-NO2	$HONO \Rightarrow OH + NO$

A6 Dry deposition, additional information

A6.1 Leaf area index calculations

Leaf area index (LAI, which is one-sided, projected) is calculated according to Table A14, making use of Table 3.

Table A14. Calculation of LAI as a function of daynumber d_n , start and end days of growing season (d_{SGS} , d_{EGS}), and other parameters as given in Table 3. See also Fig. 4

Time of year	LAI
$d_n \leq d_{SGS}$ or $d_n \geq d_{EGS}$	LAI_{\min}
$d_{SGS} < d_n \leq d_{SGS} + L_S$	$LAI_{\min} + (LAI_{\max} - LAI_{\min})(d_n - d_{SGS})/L_S$
$d_{SGS} + L_S < d_n \leq d_{EGS} - L_E$	LAI_{\max}
$d_{EGS} - L_E < d_n < d_{EGS}$	$LAI_{\min} + (LAI_{\max} - LAI_{\min})(d_{EGS} - d_n)/L_E$

A6.2 Stomatal conductance calculations

As noted in section 8.5, the calculation of stomatal conductance according to the DO₃SE algorithm requires the calculation of factors accounting for time of year (leaf phenology factor, f_{phen}), the minimum observed stomatal conductance (f_{\min}), light (PAR, with factor f_{light}), temperature (f_T), vapour-pressure deficit (D , factor f_D), and soil-water (SW, factor f_{SW}). Such functions and their parameters have been presented widely in the literature, and in LRTAP (2009). However, the values and equations have been modified over the years. Here we present the equations and parameter values used in the EMEP model. These are loosely based upon those presented in LRTAP (2009), but (especially in the case of f_{phen}) simplified somewhat to match the limitations inherent in large-scale modelling. As an important example, we have shown previously that even such basic parameters as the start of the growing season are difficult to capture with European-wide models (Tuovinen et al., 2009).

Table A15 lists g_{max} values (given at normal temperature and pressure, in $\text{mmole O}_3 \text{ m}^{-2} (\text{PLA}) \text{ s}^{-1}$, denoted g_{max}^m) along with values of other parameters needed for the conductance modelling. For pressure P and temperature T , g_{max} in m s^{-1} units is given by:

$$g_{max} = g_{max}^m R T / P \quad (\text{A8})$$

R is here the gas-constant ($8.314 \text{ J mole}^{-1} \text{ K}^{-1}$). At normal temperature and pressure, $g_{max} \approx g_{max}^m / 41000$. The canopy average stomatal conductance, g_{sto} , is calculated as:

$$g_{sto} = g_{max} f_{phen} f_{light} \max(f_{\min}, f_T f_D f_{SW}) \quad (\text{A9})$$

Table A15 gives the landcover species parameters associated with f_{phen} , f_{light} , f_T and f_D . f_{phen} is calculated according to Table A6.2, and is illustrated for two land-cover types in Fig. A1. The summertime dip in f_{phen} for the Mediterranean species is intended to reflect the well-documented effects of drought-stress on vegetation in this area, although it is an open question if this procedure is double-counted in the f_{SW} function (see Alonso et al., 2008, for contrasting examples).

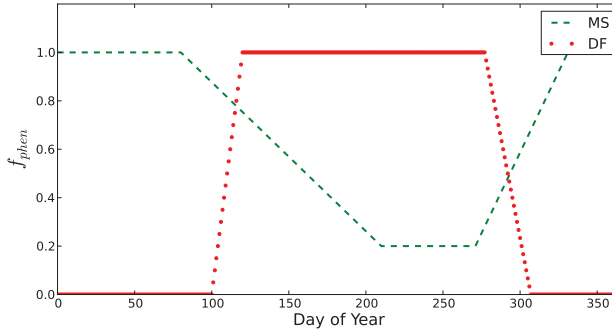


Fig. A1. Illustration of f_{phen} function for two contrasting land-cover classes, DF (temperature/boreal deciduous, here at 50° N) and (MS) Mediterranean scrub.

Table A15. Land-cover specific parameters for stomatal conductance (DO_3SE) calculations

Code	g_{max}^m	f_{min}	f_{phen} factors								f_{light}	f_T			f_D		
			ϕ_a	ϕ_b	ϕ_c	ϕ_d	ϕ_e	ϕ_f	ϕ_{A_S}	ϕ_{A_E}		α	T_{min}	T_{opt}	T_{max}	D_{max}	D_{min}
	†						days	days	days	days		°C	°C	°C	kPa	kPa	kPa
CF	140	0.1	0.8	0.8	0.8	0.8	1	1	0	0	0.006	0	18	36	0.5	3	
DF	150	0.1	0	0	1	0	20	30	0	0	0.006	0	20	35	1	3.25	
NF	200	0.1	1	1	0.2	1	130	60	80	35	0.013	8	25	38	1	3.2	
BF	200	0.02	1	1	0.3	1	130	60	80	35	0.009	1	23	39	2.2	4	
TC	300	0.01	0.1	0.1	1	0.1	0	45	0	0	0.0105	12	26	40	1.2	3.2	8
MC	300	0.019	0.1	0.1	1	0.1	0	45	0	0	0.0048	0	25	51	1	2.5	
RC	360	0.02	0.2	0.2	1	0.2	20	45	0	0	0.0023	8	24	50	0.31	2.7	10
SNL	60	0.01	1	1	1	1	1	1	0	0	0.009	1	18	36	1.3	3	
GR	270	0.01	1	1	1	1	0	0	0	0	0.009	12	26	40	1.3	3	
MS	200	0.01	1	1	0.2	1	130	60	80	35	0.012	4	20	37	1.3	3.2	
IAM_LCR	500	0.01	0.1	0.1	1	0.1	0	45	0	0	0.0105	12	26	40	1.2	3.2	8
IAM_DF	150	0.1	0	0	1	0	15	20	0	0	0.006	0	21	35	1	3.25	
IAM_MF	175	0.02	1	1	0.3	1	130	60	80	35	0.009	2	23	38	2.2	4	

Notes: † Units of g_{max}^m are $\text{mmole O}_3 \text{ m}^{-2} (\text{PLA}) \text{ s}^{-1}$

Table A16. Definition of phenology function, f_{phen} as a function of daynumber d_n , start and end of growing season (d_{SGS} , d_{EGS}), and other parameters as given in Table A15

Time of year	f_{phen}
$d_n \leq d_{SGS}$ or $d_n > d_{EGS}$	0
$d_{SGS} < d_n \leq A_{start}$	ϕ_a
$A_{start} < d_n \leq A_{start} + \phi_c$	$\phi_b + (\phi_c - \phi_b)(d_n - A_{start})/\phi_c$
$A_{start} + \phi_c < d_n \leq A_{end} - \phi_f$	ϕ_c
$A_{end} - \phi_f < d_n \leq A_{end}$	$\phi_d + (\phi_c - \phi_d)(A_{end} - d_n)/\phi_f$
$A_{end} < d_n \leq d_{EGS}$	ϕ_d

Notes: A_{start} calculated from $d_{SGS} + \phi_{A_S}$, A_{end} from $d_{EGS} - \phi_{A_E}$, c.f. Table A15.

Calculation of f_{light} makes use of the photosynthetic active radiation components, I_{PAR}^{sun} and I_{PAR}^{shade} , as presented in Sect. 4. We calculate the effects for sun and shade leaves with:

$$f_{sun} = 1 - e^{-\alpha I_{PAR}^{sun}} \quad (A10)$$

$$f_{shade} = 1 - e^{-\alpha I_{PAR}^{shade}} \quad (A11)$$

where α values are land-cover specific and given in Table A15. Given the fraction of leaves in sun ($f_{LAI}^{sun} = LAI_{sun}/LAI$, Sect. 4), the canopy average f_{light} is calculated as:

$$f_{light} = f_{LAI}^{sun} f_{sun} + (1 - f_{LAI}^{sun}) * f_{shade} \quad (A12)$$

Calculation of f_T uses the 2m air temperature T_2 , together with parameters from Table A15:

$$f_T = \frac{T_2 - T_{min}}{T_{opt} - T_{min}} \left(\frac{T_{max} - T_2}{T_{max} - T_{opt}} \right)^\beta \quad (A13)$$

where β is given by $(T_{max} - T_{opt}) / (T_{opt} - T_{min})$. f_T is set to 0.01 outside the T_{min} to T_{max} range. (All temperatures here are in °C.)

The effects of humidity are accounted for with f_D , with the basic calculation given by:

$$f_D = f_{min} + (1 - f_{min}) \frac{D_{min} - D}{D_{min} - D_{max}} \quad (A14)$$

f_D is further constrained to lie between f_{min} and 1.0.

For a few landcover categories (see Table A15), ΣD_{crit} values are specified. For these landcovers, we also calculate ΣD (h), the hourly time-integral all vapour pressure deficits from sunrise until the current hour, h. ΣD accumulates over the day, and when ΣD (h) exceeds ΣD_{crit} , then we enforce:

$$g_{sto}(h) \leq g_{sto}(h-1) \quad (A15)$$

This procedure is mainly designed to prevent afternoon g_{sto} increasing after a period of morning water stress, as suggested by Uddling et al. (2004) and LRTAP (2009).

As noted in Sect. 8.4 soil water (SW) is very difficult to model accurately in large-scale models, so we use a simple procedure which should capture some of the main effects of dry periods on g_{sto} . The exact methodology depends on the NWP model and its SW outputs, but essentially we define minimum and maximum soil water amounts to be SW_{min} (identified with wilting point in ECMWF data for example), SW_{max} (field capacity in ECMWF), and then define relative extractable water, $R_{EW} = (SW - SW_{min}) / (SW_{max} - SW_{min})$. Then:

$$f_{SW} = 1, \text{ for } R_{EW} \geq 0.5 \quad (A16)$$

$$f_{SW} = 2 R_{EW}, \text{ for } R_{EW} < 0.5$$

A6.3 Properties of gases for dry deposition

Table A17. Properties of gases for dry deposition calculations. Diffusivity ratio for a gas i , $D_r = D_{H_2O}/D_i$, Solubility index H_* (based upon Effective Henry's coefficient), and Reactivity index f_o . Based upon Wesely et al. (1985).

Gas	D_r	H_*	f_o
SO2	1.9	1.0×10^5	0.0
O3	1.6	1.0×10^{-2}	1.0
NO2	1.6	1.0×10^{-2}	0.1
HNO3	1.9	1.0×10^{14}	0.0
H2O2	1.4	1.0×10^5	1.0
HCHO	1.3	6.0×10^3	0.0
ALD ^(a)	1.6	15	0.0
OP ^(b)	1.6	2.4×10^2	0.1
NH3 ^(c)	1.0	1.0×10^5	0.0
PAN	2.6	3.6	0.1

Notes: (a) Used for all aldehydes except HCHO; (b) OP=Wesely "Methyl hydroperoxide" - used for all hydroperoxides (c) H_* increased compared to Wesely value, reflecting European pH conditions.

Table A18. Base-values of ground-surface resistance for sulphur dioxide ($\hat{R}_{gs}^{SO_2}$) and ozone ($\hat{R}_{gs}^{O_3}$). Units: s m⁻¹.

Landuse	$\hat{R}_{gs}^{SO_2}$	$\hat{R}_{gs}^{O_3}$
Forests, Mediterranean scrub	-	200
Crops	-	200
Moorland	-	400
Grasslands	-	1000
Wetlands	50	400
Tundra	500	400
Desert	1000	2000
Water	1	2000
Ice+snow	1000	2000
Urban	400	400

Notes: '-' - denotes other formulation, using resistances calculated as given in Sect. 8.7.

A7 Wet deposition, additional information

Table A19. Wet scavenging ratios and collection efficiencies used in the EMEP MSC-W model.

Components ^(a)	$W_{sm} (\times 10^6)$	$W_{sub} (\times 10^6)$	\bar{E}	Comment
SO ₂	0.3	0.15	-	
HNO ₃ , HONO, NH ₃ , H ₂ O ₂	1.4	0.5	-	
HCHO	0.1	0.03	-	
ROOH	0.05	0.015	-	
PMf	1.0	-	0.02	Generic fine particles, includes SO ₄ ²⁻ , NH ₄ ⁻ , fine-NO ₃ ⁻ , ECage_f, OA ^(b) , fine-dust
PMecf	0.2	-	0.02	Fresh (hydrophobic) ECnew_f
PMssf	1.6	-	0.02	Fine sea-salt
PMssc	1.6	-	0.4	Coarse sea-salt
PMc	1.0	-	0.4	Other coarse particles, includes coarse: NO ₃ ⁻ , PPM, dust

(a) ROOH, and PM- type components are generic labels, see also Table A5 for particles associated with these rates; (b) For semi-volatile compounds associated with organic aerosol (OA), only the particle fraction is scavenged.

A8 Initial and boundary conditions, additional information

Table A20. Parameters used to set prescribed boundary conditions

	χ_{mean}	d_{max}	$\Delta\chi$	H_z	χ_{min}^v	χ_{min}^h
	ppb	days	ppb	km	ppb	ppb
SO2	0.15	15	0.05	∞	0.15	0.03
SO4	0.15	180	0.00	1.6	0.05	0.03
NO	0.1	15	0.03	4.0	0.03	0.02
NO2	0.1	15	0.03	4.0	0.05	0.04
PAN	0.20	120	0.15	∞	0.20	0.1
CO	125.0	75	35.0	25.0	70.0	30.0
HNO ₃	0.07	180	0.03	∞	0.025	0.03
nitrate ^(a)	0.07	15	0.03	1.6	0.025	0.02
NH ₄ ⁺	0.15	180	0.0	1.6	0.5	0.03
C2H6	2.0	75	1.0	10.0	0.05	0.05
C4H10	2.0	45	1.0	6.0	0.05	0.05
HCHO	0.7	180	0.3	6.0	0.05	0.05
CH3CHO	0.3	180	0.05	6.0	0.005	0.005
Seasalt fine	0.5	15	0.3	1.6	0.01	0.01
Seasalt coarse	3.0	15	1.0	1.6	0.01	0.01

Notes: See text for definition of terms. (a) same values used for both coarse and fine nitrate. Concentrations and other parameters estimated largely from Warneck (1988); Derwent et al. (1998); Ehhalt et al. (1991); Emmons et al. (2000); Isaksen and Hov (1987); Lewis et al. (2005); Millet et al. (2010); Penkett et al. (1993); Singh et al. (2004); Solberg et al. (1996, 2001) and University of Oslo CTM2 model (Sundet, 1997).

Table A21. Latitude factors applied to prescribed boundary and initial conditions.

Component	Latitude (° N)									
	30	35	40	45	50	55	60	65	70-90	
SO2 ^a	0.05	0.15	0.3	0.8	1.0	0.6	0.2	0.12	0.05	
HNO3 ^b	1.00	1.00	1.00	0.85	0.7	0.55	0.4	0.3	0.2	
PAN	0.15	0.33	0.5	0.8	1.0	0.75	0.5	0.3	0.1	
CO	0.6	0.7	0.8	0.9	1.0	1.0	0.95	0.85	0.8	

Notes: (a) Applied also for SO₄, NO, NO₂; (b) Applied also for HCHO, CH₃CHO; See Simpson (1992) for sources of data

Table A22. Assumed trends for boundary concentrations

Species	Trend , pre-1990 %/year	Trend , post-1990 %/year	Notes
O3	1	(a)	(b)
CO	0.85	0	(c)
VOC	0.85	0	(d)
CH4	0.91	0.2	(e)

Notes: (a) Mace-head correction applied on yearly basis to climatological values from 1990-current year, see section 10.1. (b) pre-1990 from Janach (1989); Low et al. (1990); Volz and Kley (1988); Bojkov (1986); Logan (1994) (c) Trend for CO of 0.85%/yr from Zander et al. (1989b); (d) Trend for ethane of 0.85%/yr from Ehhalt et al. (1991). Same trends assumed for n-butane and ethene. (e) Pre-1990 values from Zander et al. (1989a) for 1975-1990. Post-1990 values valid for 1990-2000, derived from Mace-Head observations.